

Optical bistability with bound states in the continuum in dielectric gratings

Dmitrii N. Maksimov^{1,2}, Andrey A. Bogdanov³, and Evgeny N. Bulgakov^{1,4}

¹*Kirensky Institute of Physics, Federal Research Center KSC SB RAS, 660036, Krasnoyarsk, Russia*

²*Siberian Federal University, 660041, Krasnoyarsk, Russia*

³*Department of Physics and Engineering, ITMO University, 191002, St. Petersburg, Russia*

⁴*Reshetnev Siberian State University of Science and Technology, 660037, Krasnoyarsk, Russia*

(Dated: May 29, 2020)

We consider light scattering by dielectric gratings supporting optical bound states in the continuum. Due to the presence of instantaneous Kerr nonlinearity the critical field enhancement in the spectral vicinity of the bound state triggers the effect of optical bistability. The onset of bistability is explained theoretically in the framework of the temporal coupled mode theory. As the central result we cast the problem into the form of a singly field-driven nonlinear oscillator. The theoretical results are verified in comparison against full-wave numerical simulations.

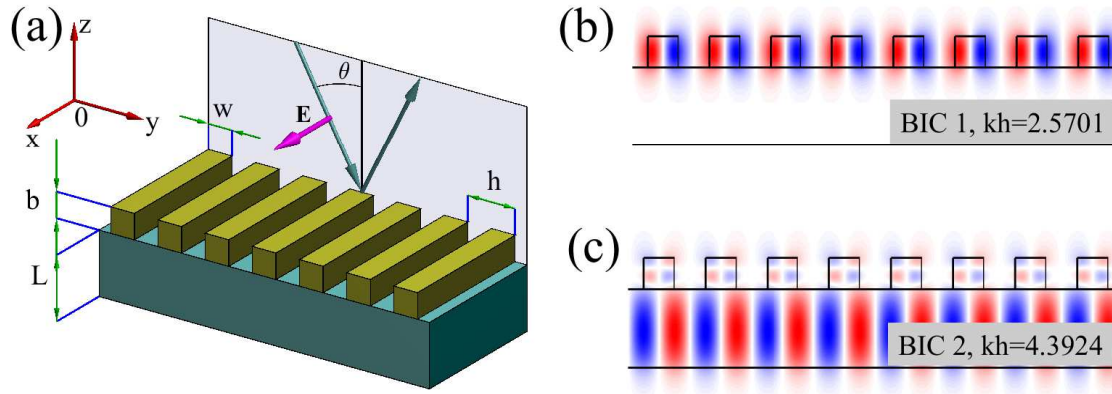


FIG. 1: (a) The dielectric grating of Si bars on glass substrate. The plane of incidence $y0z$ is shaded grey. The magenta arrow shows the electric vector of the incident wave. The parameters are $w = 0.5h$, $b = 0.5h$, $L = 1.25h$ (b, c) The electric field profiles of two symmetry protected BICs visualized as E_x in the $y0z$ plane.

I. INTRODUCTION

Engineering high-quality resonances which provide access to tightly localized optical fields has become a topic of paramount importance in electromagnetism¹⁻⁴. In that context, dielectric gratings (DGs) are a useful optical instrument with numerous applications relying on high-quality resonances^{3,5} that occur in the spectral vicinity of the avoided crossings of the DG modes⁶. The utmost case of light localization is a bound state in the continuum (BIC) - an embedded state with infinite quality factor coexisting with the scattering solutions^{4,7}. Since the seminal paper by Marinica, Borisov, and Shabanov⁸ BICs in all-dielectric DGs have been extensively studied both theoretically⁹⁻¹⁴ and experimentally^{15,16}. Lately, optical BICs have also been reported in hybrid photonic-plasmonic gratings^{17,18}.

The BICs are spectrally surrounded by a leaky band of high-quality resonances which can be excited from the far-zone¹⁹. The excitation of the strong resonances leads to critical field enhancement^{20,21} with the near-field amplitude controlled by the frequency and the angle of incidence of the incoming monochromatic wave. The critical field enhancement allows for activating nonlinear optical effects even with a small amplitude of the incident waves. Such resonant enhancement of nonlinear effects may lead to the effects of symmetry breaking²² and channel dropping²³.

Among various potential applications in nonlinear optics the BICs have been used for second harmonic (SH) generation. In particular, giant conversion efficiency into SH (up to 40%) was predicted for an array of parallel dielectric cylinders²⁴. A more practical design of AlGaAs metasurface on a quartz substrate supporting BIC was analyzed in²⁵, where the efficiency of SH generation $P_{2\omega}/P_{\omega}^2 \sim 10^{-2}$ W is predicted in the vicinity of a BIC. Recently, it was shown theoretically that BIC can enhance the SH conversion efficiency in transition-metal dichalcogenide monolayers by more than four orders of magnitude²⁶. The BIC is a dark (optically inactive) resonance which cannot be excited from the far field, however, it was shown in²⁷ that BICs in periodic dielectric structures can be excited by non-linear polarization at the SH frequency induced by the incident field. The same mechanism of destructive interference underlying BICs can result in appearance of high-quality modes in subwavelength dielectric resonators^{28,29}, which also demonstrate giant SH generation efficiency^{30,31}.

In this paper we consider the effect of the critical field enhancement on optical bistability induced by instantaneous Kerr nonlinearity. Such optical bistability emerges in the scattering spectra in the form of nonlinear Fano resonances^{32,33}. Previously the studies of optical bistability with BICs solely relied on either brute force full-wave modelling^{19,34} or phenomenological coupled-mode approach³⁵. Recently, having considered an array of nonlinear cylinders, we combined the two approaches into a single theory³⁶ that reduces the problem of finding the nonlinear response to solving a nonlinear coupled-mode equation for a single variable. Herewith all the parameters of the coupled-mode equation are known from solving the linear scattering problem in the spectral vicinity of the BIC which is a far easier task than full-wave modelling of nonlinear Maxwell's equation. In this paper, we present a generic theory applicable to planar structure with no mirror symmetry with respect to reflection in the plane of the structure. The theory is verified in comparison against full-wave numerical solutions of Maxwell's equations.

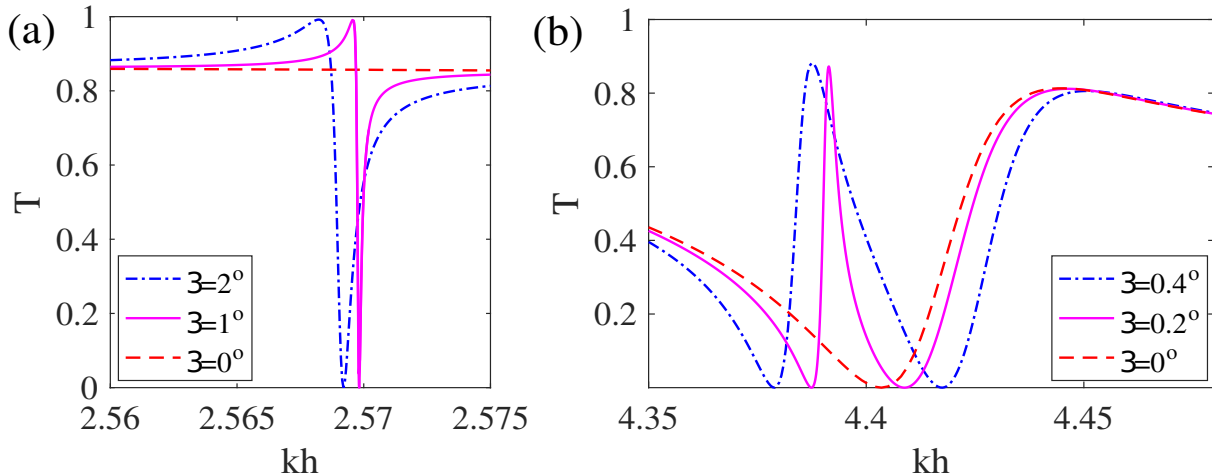


FIG. 2: (a) Transmittance spectrum in vicinity of BIC 1 at three different angles of incidence specified in the inset. (b) Transmittance spectrum in vicinity of BIC 2 at three different angles of incidence specified in the inset.

II. BOUND STATES IN THE CONTINUUM

The system under consideration is shown in Fig. 1 (a). It is a dielectric grating assembled of rectangular dielectric bars made of Si. The bars are periodically placed on the glass substrate. Here we only consider the scattering of TE polarized waves with the electric vector aligned with the Si bars as shown in Fig. 1. Under such conditions the propagation of electromagnetic waves is controlled by the Helmholtz equation for the x component of the electric field

$$\left(\frac{\partial^2}{\partial y^2} + \frac{\partial^2}{\partial z^2} \right) E_x + k^2 [n_0^2 + 2n_0 n_2 |E_x|^2] E_x = 0, \quad (1)$$

where k is the vacuum wavenumber, and $n_{0,2}$ are linear and nonlinear refractive indices, correspondingly. In what follows the refractive index of Si is taken as $n_0 = 3.575$, while the refractive index of the substrate $n_0 = 1.5$.

Our numerical simulations with the use of Dirichlet-to-Neumann map method³⁷ have demonstrated that for the set of parameters specified in the caption to Fig. 1 the system supports two in- Γ BICs coexisting with the zeroth diffraction order. The eigenmode profiles of the BICs are shown in Fig. 1 (b) and Fig. 1 (c). Notice the striking difference between BIC 1 and BIC 2 in Fig. 1 (b) and Fig. 1 (c): the field of BIC 1 is mostly localized in the Si bars, whereas the field of BIC 2 is spread across the whole grating. This difference is due to the higher eigenfrequency of BIC 2 allowing the first diffraction order in the glass substrate.

One important property of the BICs is the emergence of a collapsing Fano feature in its parametric vicinity^{38–42}. In this paper, we consider light scattering near the normal incidence so that the incident light couples to the band of resonant modes with diverging Q -factor as $\theta \rightarrow 0$. In Fig. 2 (a) and Fig. 2 (b) we show the transmittance spectra in the spectral vicinity of BIC 1 and BIC 2, correspondingly. One can see that in both cases one observes a narrow Fano feature which collapses at the exact normal incidence. There is also a difference between the two cases. Namely, there is more than a single Fano resonance at BIC 2. The transmittance exhibits two zeros and an extra peak which does not vanish at the normal incidence. This difference can be explained through different nature of BIC 1 and BIC 2. One can see from Fig. 2 that BIC 1 occurs as an isolated resonance, while BIC 2 emerges as a result of hybridisation of two resonant modes with one of them acquiring infinite life-time. The latter mechanism of BIC has been previously demonstrated for dielectric gratings in¹¹. In the next section we provide a theoretical description of the lineshapes of the Fano anomalies induced by the BICs extended to the effects of Kerr nonlinearity triggered by critical field enhancement.

III. SCATTERING THEORY

The aim of this section is to formulate the equation for the amplitude of the quasi-BIC resonant mode in the framework of the temporal coupled mode theory (TCMT)⁴³. The generic case of a TCMT applied to a 2D structure

is considered in⁴⁴. It has been demonstrated that in the absence of mirror symmetry with respect to $y \rightarrow -y$ the application of TCMT requires considering four scattering channels. However, as the above symmetry holds in our case, we shall apply a two-channel TCMT in this paper. Following³⁶ we only consider the effect of a single resonant mode mentioning in passing that a generalization of the TCMT to multimodal case is possible⁴⁵.

A. Coupled mode approach

Let us start with the TCMT equation for an isolated resonance⁴³

$$\frac{da(t)}{dt} = i(\omega_0 - \Gamma)a + \langle d^* | s^{(+)} \rangle, \quad (2)$$

where $a(t)$ is the time-dependent amplitude of the resonant mode, ω_0 is the resonant frequency, Γ is the inverse life-time of the resonance, $|d\rangle$ is the vectors of coupling constants to the scattering channels, and $|s^{(+)}\rangle$ is the vector of incident amplitudes. Since we stay in the domain where only specular reflection is allowed, both $|s^{(+)}\rangle = (s_1^{(+)}, s_2^{(+)})^\top$, and $|d\rangle = (d_1, d_2)^\top$ are 2×1 vectors. The subscripts 1, 2 are applied to the upper and lower half-spaces, correspondingly. Let us, e.g., assume that a monochromatic plane wave with frequency ω is incident onto the grating from the upper half-space. The vector of the incident amplitudes is written as

$$|s^{(+)}\rangle = \left(\sqrt{I_0}, 0 \right)^\top, \quad (3)$$

where I_0 is the flux density supported by the incident wave. After the time-harmonic substitution $a(t) = ae^{i\omega t}$ one finds

$$a = \frac{d_1 \sqrt{I_0}}{[i(\omega - \omega_0) + \Gamma]}. \quad (4)$$

Finally, the outgoing amplitudes can be found from the following equation

$$|s^{(-)}\rangle = \widehat{C} + a|d\rangle. \quad (5)$$

Here, \widehat{C} is the matrix of direct (non-resonant) process. In the case of the symmetry protected BIC, the matrix \widehat{C} can be easily obtained numerically by solving the scattering problem at the normal incidence with the incident frequency equal to the BIC frequency. In the other words exactly in the point of the Fano resonance collapse³⁶.

The general solution of the linear scattering problem can be written through the scattering matrix $\widehat{S}(\omega)$ which links the vectors of incident and outgoing amplitudes

$$|s^{(-)}\rangle = \widehat{S}(\omega)|s^{(+)}\rangle. \quad (6)$$

Since the system under consideration is both energy preserving and symmetric with respect to time reversal, the matrices $\widehat{S}(\omega)$ and \widehat{C} are simultaneously unitary and symmetric⁴⁶. The most generic form of \widehat{C} can be parameterized in the following manner

$$\widehat{C} = e^{i\phi} \begin{pmatrix} \rho e^{-i\eta} & i\tau \\ i\tau & \rho e^{i\eta} \end{pmatrix}, \quad (7)$$

where the real valued ρ and τ are the absolute values of the reflection and transmission amplitudes which have to satisfy the following equation

$$\rho^2 + \tau^2 = 1. \quad (8)$$

Thus, taking the above into account we are left with only three independent parameters, θ, η , and ρ which can be analytically derived from Eq. (7).

The quantities \widehat{C} and $|d\rangle$ are linked through the following equation⁴³

$$\widehat{C}|d^*\rangle = -|d\rangle, \quad (9)$$

which is a consequence of both energy conservation and time-reversal symmetry. Equation (9) constitutes a homogeneous algebraic equation for unknown $|d\rangle$. Since the complex conjugation is involved in Eq. (9) it has to be solved for

four independent variables, i.e. the real and imaginary parts of $|d\rangle$. This results in a system of four equations of rank 2. Therefore the general solution of Eq. (9) can be written as a function of two independent parameters α and β .

$$|d\rangle = \begin{pmatrix} (\tau\alpha - i(1+\rho)\beta)e^{i\frac{\phi-\eta}{2}} \\ (\tau\beta - i(1+\rho)\alpha)e^{i\frac{\phi+\eta}{2}} \end{pmatrix}. \quad (10)$$

Notice that in general $d_1 \neq d_2$. Thus, Eq. (10) takes into account the asymmetry of the coupling to the upper and lower half-spaces due to the lack of mirror symmetry in the plane of the structure, see Fig. 1 (a).

Another important relationship⁴³ is also a consequence of energy conservation

$$2\Gamma = \langle d|d\rangle. \quad (11)$$

The above equation is derived by considering the decay dynamics of the system with no impinging wave. Assume that a certain amount of energy E is loaded into the resonant mode, then the solution of Eq. (2) $a(t) = a(0)e^{i\omega_0 t - \Gamma t}$. Given that the eigenmode stores a unit energy, the energy dissipation rate can be found as

$$\frac{d\mathcal{E}}{dt} = -2\Gamma|a_0|^2, \quad (12)$$

where \mathcal{E} is the energy stored in the resonant eigenmode. On the other hand if each scattering channel attenuates a unit of energy per unit of time, Eq. (6) yields

$$\frac{d\mathcal{E}}{dt} = -\langle d|d\rangle|a_0|^2. \quad (13)$$

Combining Eqs. (12) and (13) we find Eq. (11). Notice, that normalization of both the eigenmode and decay channels is important for deriving Eq. (11). Application of Eq. (11) to Eq. (10) yields

$$\alpha^2 + \beta^2 = \frac{2\Gamma}{\tau^2 + (1+\rho)^2}. \quad (14)$$

Let us summarize the findings of this subsection. First, as it is seen from Eq. (4) the resonant response is due to vanishing Γ in denominator. Notice that both Γ and ω_0 are known from the eigenmode spectrum of the grating, they can be determined as the real and imaginary part of the resonant frequency of the leaky band host the BIC, as it has been done in³⁶. Second, the coupling vector $|d\rangle$ is defined from the matrix of the direct process Eq. (7) via Eq. (10) up to two unknown real-valued parameters. Quite remarkable is that the presence of a symmetry protected BIC gives an easy access to the matrix of the direct process by simply computing the scattering solution at the BIC frequency and the normal incidence³⁶. Finally, Eq. (14) allows for eliminating one of the free parameters, say α in Eq. (10). The remaining parameter β can be found by easily found by fitting the transmittance spectrum found through the full-wave solution of the scattering problem.

B. Green's function

Let us now generalize the above result to the system with Kerr nonlinearity. In this subsection we apply the resonant state expansion method⁴⁷ for deriving the TCMT equation with account of nonlinearity. The key figure of merit in the resonant state expansion method is Green's function of Maxwell's equations. According to⁴⁷ the spectral representation of Green's function can be written as

$$G(\mathbf{r}', \mathbf{r}, k_0, k_y) = \sum_n \int \frac{E_x^{(n)}(\mathbf{r}, k_y) E_x^{(n)}(\mathbf{r}', -k_y)}{2k[k - k_n(k_y)]}, \quad (15)$$

where $E_x^{(n)}(\mathbf{r}, k_y)$ the field profile of the n th resonant eigenmode and $k_n(k_y)$ is the dispersion of the resonant eigenfrequency of the leaky band in terms of vacuum wave number, $k = \omega/c$ with c as the speed of light. The symbol \sum_n is used for the combined contribution of a discrete sum and integration along the cuts. For the spectral representation Eq. (15) to be valid the eigenfields $E_x^{(n)}(\mathbf{r}, k_y)$ must obey the following normalization condition

$$1 + \delta_{0,k_n} = I_n^V + \lim_{k \rightarrow k_n} \frac{S_n^{\theta V}}{k^2 - k_n^2} \quad (16)$$

with

$$I_n^V = \int_V dV E_x^{(n)}(\mathbf{r}, -k_y) E_x^{(n)}(\mathbf{r}', k_y) \quad (17)$$

and

$$S_n^{\partial V} = \oint_{\partial V} dS \left[E_x^{(n)}(\mathbf{r}, -k_y) \partial_S \tilde{E}_x^{(n)}(\mathbf{r}', k_y, k) - \tilde{E}_x^{(n)}(\mathbf{r}, -k_y, k) \partial_S E_x^{(n)}(\mathbf{r}', k_y) \right], \quad (18)$$

where ∂_S is used for the normal derivative with respect to the boundary of the elementary cell and $\tilde{E}_z^{(n)}(\mathbf{r}', k_y, k_0)$ is the analytic continuation of the eigenfield in the vicinity of its resonant eigenfrequency such as

$$E_x^{(n)}(\mathbf{r}', k_y) = \lim_{k \rightarrow k_n} \tilde{E}_x^{(n)}(\mathbf{r}', k_y, k). \quad (19)$$

C. Resonant approximation

To establish a link between the resonant state expansion and the single mode TCMT we apply resonant approximation, i.e. in Eq. (15) we retain only the term with $k - k_n(k_y)$ in the denominator. All the other terms are assumed to be independent of frequency on the scale of the narrow Fano feature induced by the BIC. In terms of the TCMT the non-resonant terms are accumulated into the direct process. The resulting resonant Green's function is simply

$$G^{(\text{res})}(\mathbf{r}', \mathbf{r}') = \frac{E_x^{(0)}(\mathbf{r}, k_y) E_x^{(0)}(\mathbf{r}', -k_y)}{2k[k - k(k_x)]}, \quad (20)$$

where $E_x^{(0)}(\mathbf{r}, k_y)$ is the profile of the resonant eigenmode. Above we omitted the band index of the dispersion $k(k_x)$ bearing in mind that the resonant approximation uses the dispersion and the mode profiles of the BIC host band.

At first let us again consider linear scattering problem. As before we assume that a TE polarized plane wave with intensity I_0 impinges onto the structure at the near normal incidence. Then, solving Eq. (1) with the resonant Green's function Eq. (20) one finds

$$E_x = \frac{\sqrt{I_0} E_x^{(0)}(\mathbf{r}, k_y)}{2k[k - k(k_y)]} \int_V dV E_x^{(0)}(\mathbf{r}', -k_y) J(\mathbf{r}'), \quad (21)$$

where the source term can be express through the incident field $E_x^{(\text{in})}$ as

$$J = - \left(\frac{\partial^2}{\partial y^2} + \frac{\partial^2}{\partial z^2} \right) E_x^{(\text{in})} - n_0^2 E_x^{(\text{in})}, \quad (22)$$

where $E_x^{(\text{in})}$ is normalized to carry a unit of energy per unit of time per unit are of the boundary of the scattering domain. Thus, amplitude of the physical incident wave is only controlled by I_0 .

To be consistent with the resonant approximation we also assume that the near-field response is dominated by the quasi-BIC eigenmode

$$E_x = \frac{1}{\sqrt{A}} a E_x^{(0)}, \quad (23)$$

where A is the normalization constant. Substituting the above equation into Eq. (21) one finds

$$a = \frac{\sqrt{I_0 A}}{2k[k - k(k_x)]} \int_V dV E_x^{(0)}(\mathbf{r}', -k_y) J(\mathbf{r}'). \quad (24)$$

By comparing Eqs. (4) and (24) one finds

$$d_1 = \frac{i\sqrt{A}c}{2k} \int_V dV E_x^{(0)}(\mathbf{r}', -k_y) J(\mathbf{r}'), \quad (25)$$

where c is the speed of light. The above equation is difficult to be applied in computations, since it requires the explicit analytic form of the leaky mode profiles under normalization condition Eq. (16). We, however, already know from the previous subsection how d_1 can be found from the scattering spectra with the use of Eqs. (10) and (14).

D. Nonlinear case

Now let us generalize the above result onto the non-linear case. After taking the same route we end up with the following equation for a

$$a + \mathcal{J} \frac{n_0 n_2 k}{A[k - k(k_y)]} |a|^2 a = \frac{\sqrt{I_0} d_1}{ic[k - k(k_y)]}, \quad (26)$$

where

$$\mathcal{J} = \int_{V_{\text{non}}} dV E_x^{(0)}(-k_y) E_x^{(0)}(k_y) |E_x^{(0)}(k_y)|^2, \quad (27)$$

and the integration is performed only over the domain with nonlinear refractive index V_{non} . Finally notice that \mathcal{J} must be parabolic in k_y , since the problem is symmetric with respect to the angle of incidence. Therefore we drop the dependence on k_y using the field profile in the Γ -point, i.e. the BIC

$$\mathcal{J} = \int_{V_{\text{non}}} dV |E_x^{(\text{BIC})}|^4 + \mathcal{O}(k_y^2). \quad (28)$$

Since the BIC profile is a well behaved function decaying with the distance from the grating. Following⁴⁸ one easily finds that Eq. (16) is equivalent to the integration over z from plus to minus infinity

$$1 = \int_{-\infty}^{\infty} dV n_0^2 |E_x^{(\text{BIC})}|^2. \quad (29)$$

Importantly, Eq. (29) does not contain surface terms and, thus, can be easily implemented in simulations taking into account that the BIC decays exponentially with $|z| \rightarrow \infty$. Finally, notice that the integral in Eq. (29) is equal to twice electromagnetic energy stored in the BIC. Thus, to be consistent with Eq. (11) we set $A = 2$.

E. Nonlinear temporal coupled mode equation

Now, in accordance with Eq. (26) the final result reads

$$[i(\omega - \omega_0) + \Gamma]a + i\frac{\mathcal{J}}{2} n_0 n_2 \omega |a|^2 a = \sqrt{I_0} d_1. \quad (30)$$

Equation (30) only differs from Eq. (4) by the presence of nonlinear term proportional to J . It means that for describing the nonlinear response in the spectral vicinity of a BIC it is sufficiently to know the solution of the linear problem including the field profile of the BIC. Once the BIC field profile is known it can be substituted into Eq. (28) to find \mathcal{J} . The nonlinear Eq. (30) can be then solved for the response in the frequency domain.

It is remarkable that the nonlinear correction in Eq. (30) exactly coincides with that obtained previously with the perturbation theory⁴⁹. Notice, however, that the results reported in⁴⁹ have been obtained under assumption of smallness of the nonlinear term. Another issue with straightforward application of the perturbation theory is the normalization condition of the unperturbed eigenmodes. The formal solution presented in⁴⁹ involves integration across the whole space which is impossible due to divergence of the resonant eigenmodes in the far zone⁵⁰. As one can see from the previous subsection the normalization issue can only be easily resolved in the spectral vicinity of a BIC.

Finally, in the time domain Eq. (30) can be replaced by

$$\frac{d}{dt} \left(a + \frac{\mathcal{J}}{2} n_0 n_2 |a|^2 a \right) = (i\omega_0 - \Gamma)a + \sqrt{I_0} d_1 e^{i\omega t}. \quad (31)$$

The time-harmonic solutions of the above equations can be tested for stability by series expansions with respect to small perturbation as explained in³⁶.

IV. NUMERICAL VALIDATION

In this section we apply our previous findings to the scattering spectra. To obtain the matrices of the direct process we numerically solved the linear scattering problem at exact normal incidence with the vacuum wave number of the

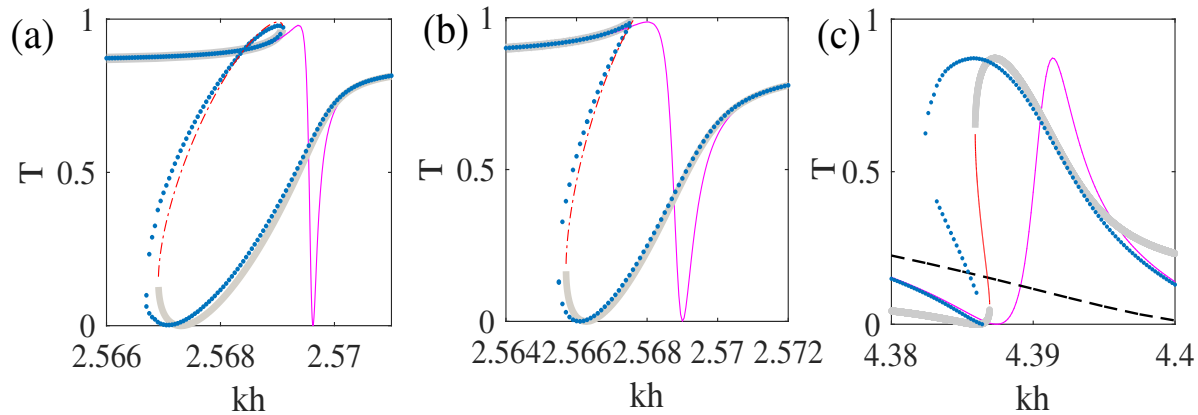


FIG. 3: Bistability in transmittance spectra. (a) BIC 1, $\theta = 1^\circ$, $I_0 = 1.82 \cdot 10^5$ MW/m². (b) BIC 1, $\theta = 2^\circ$, $I_0 = 8.39 \cdot 10^5$ MW/m². (c) BIC 2, $\theta = 0.2^\circ$, $I_0 = 3.92 \cdot 10^8$ MW/m². The thin magenta lines demonstrate Fano resonances unperturbed by the nonlinearity. The blue dots are full-wave numerical solutions obtained with pseudospectral method. The stable solutions of Eq. (30) are shown by thick grey lines. Thin red lines show unstable solutions of Eq. (30). Dashed black line in (c) show the transmittance at exact normal incidence.

incident wave equal to that of the BIC. For BIC 1 the following matrix of the direct process has been found

$$\hat{C}_{\text{BIC1}} = \begin{pmatrix} -0.3753 + 0.0494i & -0.8834 + 0.2765i \\ -0.8833 + 0.2765i & 0.3365 - 0.1734i \end{pmatrix}, \quad (32)$$

while for BIC 2 the numbers are

$$\hat{C}_{\text{BIC2}} = \begin{pmatrix} -0.9333 - 0.1121i & 0.0768 - 0.3323i \\ 0.0768 - 0.3323i & -0.8879 - 0.3086i \end{pmatrix}. \quad (33)$$

In the next step the numerical values of the three remaining parameters ω_0 , Γ , and α were evaluated by fitting to the scattering spectra in Fig. 2 at different angles of incidence. The effective nonlinearity coefficient was found with Eq. (28) by integrating the BIC profiles shown in Fig. 1 (b), and Fig. 1 (c). The results are collected in Table 1. In Table 1 we also present the ratio of the absolute values of the coupling constants d_1 and d_2 . One can see that in both cases the coupling to the lower half-space is somewhat larger than to the upper half-space, $|d_1| < |d_2|$.

TABLE I: List of the TCMT parameters.

	θ	$h\omega_0/c$	$h\Gamma/c$	α (p.d.u.)	$ d_1/d_2 $	\mathcal{J} (p.d.u.)
BIC 1	1°	2.5670	$0.065 \cdot 10^{-5}$	$6.24 \cdot 10^{-3}$	0.907	$3.04 \cdot 10^{-2}$
BIC 1	2°	2.5689	$0.031 \cdot 10^{-3}$	$1.23 \cdot 10^{-2}$	0.914	$3.04 \cdot 10^{-2}$
BIC 2	0.2°	4.39074	$1.59 \cdot 10^{-3}$	$9.05 \cdot 10^{-2}$	0.717	$3.79 \cdot 10^{-4}$

To obtain the nonlinear scattering spectra Eq. (1) was solved numerically with the pseudospectral method⁵¹. In our simulations we took $n_2 = 5 \cdot 10^{-18}$ m²/W which corresponds to silicon at $1.8 \mu\text{m}$ ⁵². The results are plotted in Fig. 3 in comparison with numerical solution of Eq. (30). The intensities of the incident waves are given in the caption to Fig. 3. First of all one can see in Fig. 3 (a) and Fig. 3 (b) that there is a reasonably good agreement between the TCM and the full-wave spectra for BIC 1. The agreement can be made perfect by slightly tuning α and/or \mathcal{J} . For BIC 2, however, the agreement is not that good and our theory can only provide a rough estimate of the parameter values leading to optical bistability. The discrepancy is due to the single-mode approximation which is not capable to account for all features of the BIC emerging with an avoided crossing. To highlight the limitations of the single-mode

TCMT in Fig. 3 (c) we plotted the transmittance at the normal incidence. One can easily see that the transmittance at the normal incidence is dependent on frequency, whereas the single-mode TCMT assumes that it is constant. On the other hand, even the single-mode approximation manages to grasp the major feature of BIC 2 with respect to initiating bistability. One can see from Table 1 that the effective nonlinearity coefficient \mathcal{J} is two orders of magnitude smaller with BIC 2 than with BIC 1. The reason for this is clearly seen from Fig. 1 (b) and Fig. 1 (c) - the field of BIC 1 is concentrated about the nonlinear medium (silicon bars), while for BIC 2 the field is evenly spread across the whole grating. The small value of \mathcal{J} results in very high intensities needed to trigger optical bistability. This rules out application of BIC 2 in a realistic experiment.

V. SUMMARY AND CONCLUSIONS

In this paper we considered the effect of optical bistability induced by bound states in the continuum (BICs) in dielectric gratings. We proposed a coupled mode approach which leads to a single nonlinear equation for the amplitude of the resonant eigenmode of the BICs host band. It is shown how all parameters entering the nonlinear coupled mode equation can be evaluated from the solution of the linear scattering problem.

We believe that the approach presented here can be of use in engineering photonic systems with the resonantly enhanced nonlinear response, as the coupled mode equation is much easier to get solved than nonlinear Maxwell's equations. At the same time our approach gives a cue for choosing the type of BICs in order to maximize the nonlinear effect. Namely, it has been shown that the BIC with the frequency lower than the first diffraction order in the substrate are better in activating the nonlinearity.

On the other hand, from the fundamental view point we have seen that the scattering of light in the spectral vicinity of a BIC can be handled by the resonant state expansion method⁴⁷. This naturally prompts us to extend the theory for the two-mode case which potentially leads to an intricate interplay between the BICs and the other mode with a finite live-time that can be excited from the far zone even at the normal incidence³⁵. The application of resonant state expansion to finite-lived states would, however, require introducing the analytical continuation normalization condition, Eq. (19) to eigenmodes that are known only numerically. We speculate that the above problem can be an interesting topic for future studies.

ACKNOWLEDGMENTS

This work was financially supported by the Government of the Russian Federation through the ITMO Fellowship and Professorship Program.

-
- ¹ Sajeev John, "Why trap light?" *Nature Materials* **11**, 997–999 (2012).
 - ² David Marpaung, Chris Roeloffzen, René Heideman, Arne Leinse, Salvador Sales, and José Capmany, "Integrated microwave photonics," *Laser & Photonics Reviews* **7**, 506–538 (2013).
 - ³ Pengfei Qiao, Weijian Yang, and Connie J. Chang-Hasnain, "Recent advances in high-contrast metastructures, metasurfaces, and photonic crystals," *Advances in Optics and Photonics* **10**, 180–245 (2018).
 - ⁴ Chia Wei Hsu, Bo Zhen, A. Douglas Stone, John D. Joannopoulos, and Marin Soljačić, "Bound states in the continuum," *Nature Reviews Materials* **1**, 16048 (2016).
 - ⁵ Connie J. Chang-Hasnain and Weijian Yang, "High-contrast gratings for integrated optoelectronics," *Advances in Optics and Photonics* **4**, 379–440 (2012).
 - ⁶ Vadim Karagodsky, Christopher Chase, and Connie J Chang-Hasnain, "Matrix fabry-perot resonance mechanism in high-contrast gratings," *Optics letters* **36**, 1704–1706 (2011).
 - ⁷ Kirill Koshelev, Gael Favraud, Andrey Bogdanov, Yuri Kivshar, and Andrea Fratalocchi, "Nonradiating photonics with resonant dielectric nanostructures," *Nanophotonics* **8**, 725–745 (2019).
 - ⁸ D. C. Marinica, A. G. Borisov, and S. V. Shabanov, "Bound states in the continuum in photonics," *Physical Review Letters* **100**, 183902 (2008).
 - ⁹ Francesco Monticone and Andrea Alù, "Bound states within the radiation continuum in diffraction gratings and the role of leaky modes," *New Journal of Physics* **19**, 093011 (2017).
 - ¹⁰ E. N. Bulgakov, D. N. Maksimov, P. N. Semina, and S. A. Skorobogatov, "Propagating bound states in the continuum in dielectric gratings," *Journal of the Optical Society of America B* **35**, 1218–1222 (2018).
 - ¹¹ Evgeny N. Bulgakov and Dmitrii N. Maksimov, "Avoided crossings and bound states in the continuum in low-contrast dielectric gratings," *Physical Review A* **98**, 053840 (2018).
 - ¹² Sun-Goo Lee and Robert Magnusson, "Band dynamics of leaky-mode photonic lattices," *Optics Express* **27**, 18180 (2019).

- ¹³ Dmitry A. Bykov, Evgeni A. Bezus, and Leonid L. Doskolovich, “Coupled-wave formalism for bound states in the continuum in guided-mode resonant gratings,” *Physical Review A* **99**, 063805 (2019).
- ¹⁴ Xingwei Gao, Bo Zhen, Marin Soljačić, Hongsheng Chen, and Chia Wei Hsu, “Bound states in the continuum in fiber bragg gratings,” *ACS Photonics* **6**, 2996–3002 (2019).
- ¹⁵ Zarina F. Sadrieva, Ivan S. Sinev, Kirill L. Koshelev, Anton Samusev, Ivan V. Iorsh, Osamu Takayama, Radu Malureanu, Andrey A. Bogdanov, and Andrei V. Lavrinenko, “Transition from optical bound states in the continuum to leaky resonances: Role of substrate and roughness,” *ACS Photonics* **4**, 723–727 (2017).
- ¹⁶ Hafez Hemmati and Robert Magnusson, “Resonant dual-grating metamembranes supporting spectrally narrow bound states in the continuum,” *Advanced Optical Materials* **7**, 1900754 (2019).
- ¹⁷ Shaimaa I. Azzam, Vladimir M. Shalaev, Alexandra Boltasseva, and Alexander V. Kildishev, “Formation of bound states in the continuum in hybrid plasmonic-photonic systems,” *Physical Review Letters* **121**, 253901 (2018).
- ¹⁸ R Kikkawa, M Nishida, and Y Kadoya, “Polarization-based branch selection of bound states in the continuum in dielectric waveguide modes anti-crossed by a metal grating,” *New Journal of Physics* **21**, 113020 (2019).
- ¹⁹ Lijun Yuan and Ya Yan Lu, “Strong resonances on periodic arrays of cylinders and optical bistability with weak incident waves,” *Physical Review A* **95**, 023834 (2017).
- ²⁰ Jae Woong Yoon, Seok Ho Song, and Robert Magnusson, “Critical field enhancement of asymptotic optical bound states in the continuum,” *Scientific Reports* **5**, 18301 (2015).
- ²¹ V. Mocella and S. Romano, “Giant field enhancement in photonic resonant lattices,” *Physical Review B* **92**, 155117 (2015).
- ²² Evgeny Bulgakov, Konstantin Pichugin, and Almas Sadreev, “Symmetry breaking for transmission in a photonic waveguide coupled with two off-channel nonlinear defects,” *Physical Review B* **83**, 045109 (2011).
- ²³ Evgeny Bulgakov, Konstantin Pichugin, and Almas Sadreev, “Channel dropping via bound states in the continuum in a system of two nonlinear cavities between two linear waveguides,” *Journal of Physics: Condensed Matter* **25**, 395304 (2013).
- ²⁴ Friends R Ndangali and Sergei V Shabanov, “The resonant nonlinear scattering theory with bound states in the radiation continuum and the second harmonic generation,” in *Active Photonic Materials V*, Vol. 8808 (International Society for Optics and Photonics, 2013) p. 88081F.
- ²⁵ Kirill Koshelev, Andrey Bogdanov, and Yuri Kivshar, “Meta-optics and bound states in the continuum,” *Science Bulletin* **64**, 836–842 (2019).
- ²⁶ Tiecheng Wang and Shihao Zhang, “Large enhancement of second harmonic generation from transition-metal dichalcogenide monolayer on grating near bound states in the continuum,” *Optics express* **26**, 322–337 (2018).
- ²⁷ Lijun Yuan and Ya Yan Lu, “Excitation of bound states in the continuum via second harmonic generations,” *SIAM Journal on Applied Mathematics* **80**, 864–880 (2020).
- ²⁸ Mikhail V Rybin, Kirill L Koshelev, Zarina F Sadrieva, Kirill B Samusev, Andrey A Bogdanov, Mikhail F Limonov, and Yuri S Kivshar, “High-q supercavity modes in subwavelength dielectric resonators,” *Physical review letters* **119**, 243901 (2017).
- ²⁹ Andrey A Bogdanov, Kirill L Koshelev, Polina V Kapitanova, Mikhail V Rybin, Sergey A Gladyshev, Zarina F Sadrieva, Kirill B Samusev, Yuri S Kivshar, and Mikhail F Limonov, “Bound states in the continuum and fano resonances in the strong mode coupling regime,” *Advanced Photonics* **1**, 016001 (2019).
- ³⁰ Luca Carletti, Kirill Koshelev, Costantino De Angelis, and Yuri Kivshar, “Giant nonlinear response at the nanoscale driven by bound states in the continuum,” *Physical review letters* **121**, 033903 (2018).
- ³¹ Kirill Koshelev, Sergey Kruk, Elizaveta Melik-Gaykazyan, Jae-Hyuck Choi, Andrey Bogdanov, Hong-Gyu Park, and Yuri Kivshar, “Subwavelength dielectric resonators for nonlinear nanophotonics,” *Science* **367**, 288–292 (2020).
- ³² Andrey E. Miroschnichenko, Sergei F. Mingaleev, Sergej Flach, and Yuri S. Kivshar, “Nonlinear Fano resonance and bistable wave transmission,” *Physical Review E* **71**, 036626 (2005).
- ³³ Stephen P Shipman and Stephanos Venakides, “An exactly solvable model for nonlinear resonant scattering,” *Nonlinearity* **25**, 2473–2501 (2012).
- ³⁴ Lijun Yuan and Ya Yan Lu, “Diffraction of plane waves by a periodic array of nonlinear circular cylinders,” *Physical Review A* **94**, 013852 (2016).
- ³⁵ S. D. Krasikov, A. A. Bogdanov, and I. V. Iorsh, “Nonlinear bound states in the continuum of a one-dimensional photonic crystal slab,” *Physical Review B* **97**, 224309 (2018).
- ³⁶ Evgeny N. Bulgakov and Dmitrii N. Maksimov, “Nonlinear response from optical bound states in the continuum,” *Scientific Reports* **9**, 7153 (2019).
- ³⁷ Yuexia Huang and Ya Yan Lu, “Scattering from periodic arrays of cylinders by dirichlet-to-neumann maps,” *Journal of Lightwave Technology* **24**, 3448–3453 (2006).
- ³⁸ Chang Sub Kim, Arkady M Satanin, Yong S Joe, and Ronald M Cosby, “Resonant tunneling in a quantum waveguide: Effect of a finite-size attractive impurity,” *Physical Review B* **60**, 10962 (1999).
- ³⁹ Stephen P Shipman and Stephanos Venakides, “Resonant transmission near nonrobust periodic slab modes,” *Physical Review E* **71**, 026611 (2005).
- ⁴⁰ Almas F Sadreev, Evgeny N Bulgakov, and Ingrid Rotter, “Bound states in the continuum in open quantum billiards with a variable shape,” *Physical Review B* **73**, 235342 (2006).
- ⁴¹ Cédric Blanchard, Jean-Paul Hugonin, and Christophe Sauvan, “Fano resonances in photonic crystal slabs near optical bound states in the continuum,” *Physical Review B* **94**, 155303 (2016).
- ⁴² E. N. Bulgakov and D. N. Maksimov, “Optical response induced by bound states in the continuum in arrays of dielectric spheres,” *Journal of the Optical Society of America B* **35**, 2443 (2018).

- ⁴³ Shanhui Fan, Wonjoo Suh, and J. D. Joannopoulos, “Temporal coupled-mode theory for the fano resonance in optical resonators,” *Journal of the Optical Society of America A* **20**, 569 (2003).
- ⁴⁴ Hengyun Zhou, Bo Zhen, Chia Wei Hsu, Owen D. Miller, Steven G. Johnson, John D. Joannopoulos, and Marin Soljačić, “Perfect single-sided radiation and absorption without mirrors,” *Optica* **3**, 1079 (2016).
- ⁴⁵ Wonjoo Suh, Zheng Wang, and Shanhui Fan, “Temporal coupled-mode theory and the presence of non-orthogonal modes in lossless multimode cavities,” *IEEE Journal of Quantum Electronics* **40**, 1511–1518 (2004).
- ⁴⁶ Zhixin Zhao, Cheng Guo, and Shanhui Fan, “Connection of temporal coupled-mode-theory formalisms for a resonant optical system and its time-reversal conjugate,” *Physical Review A* **99**, 033839 (2019).
- ⁴⁷ T. Weiss, M. Schäferling, H. Giessen, N. A. Gippius, S. G. Tikhodeev, W. Langbein, and E. A. Muljarov, “Analytical normalization of resonant states in photonic crystal slabs and periodic arrays of nanoantennas at oblique incidence,” *Physical Review B* **96**, 045129 (2017).
- ⁴⁸ Pavel S Pankin, Dmitrii N Maksimov, Kuo-Ping Chen, and Ivan V Timofeev, “Fano feature induced by a bound state in the continuum via resonant state expansion,” arXiv preprint arXiv:2003.09079 (2020).
- ⁴⁹ Jorge Bravo-Abad, Shanhui Fan, Steven G. Johnson, John D. Joannopoulos, and Marin Soljacic, “Modeling nonlinear optical phenomena in nanophotonics,” *Journal of Lightwave Technology* **25**, 2539–2546 (2007).
- ⁵⁰ Philippe Lalanne, Wei Yan, Kevin Vynck, Christophe Sauvan, and Jean-Paul Hugonin, “Light interaction with photonic and plasmonic resonances,” *Laser & Photonics Reviews* **12**, 1700113 (2018).
- ⁵¹ Lijun Yuan and Ya Yan Lu, “Efficient numerical method for analyzing optical bistability in photonic crystal microcavities,” *Optics Express* **21**, 11952 (2013).
- ⁵² Yang Yue, Lin Zhang, Hao Huang, R. G. Beausoleil, and A. E. Willner, “Silicon-on-nitride waveguide with ultralow dispersion over an octave-spanning mid-infrared wavelength range,” *IEEE Photonics Journal* **4**, 126–132 (2012).